

# A comparative study of the lime mortar used for a XIX century masonry bridge located in Cali, Colombia

JORGE GALINDO DÍAZ  
JUAN DAVID CAÑÓN  
PEDRO JOSÉ ARANGO

*Universidad Nacional de Colombia*  
Email: jagalindod@unal.edu.co

## Abstract

Two types of lime mortar (glue and plaster) have been characterized, and these types of lime mortar were used in the construction of masonry bridges, called Puente Calicanto or Puente Ortiz, which are located in Cali (Colombia) and were put into service in 1845. To this end, the techniques of X-ray Diffraction (XRD), Infrared Spectroscopy by Fourier Transform (FT-IR), Scanning Electron Microscopy (SEM) and Differential Scanning Calorimetry (DSC) have been employed. Using these different techniques, it can be concluded that each of these mortars exhibit differences in the proportion of their constituent materials, and the successful use of empirical knowledge can be demonstrated in the selection of the types of lime used by the builders. XRD characterization is adequate when crystalline phases are present, but for low-crystallinity materials, FT-IR analysis and DSC are more appropriate.

1

*Keywords:* Historic Mortar, Analytical Characterization, Historical Bridges.

## Introduction

In Colombia, construction with lime mortar was common throughout virtually the entire Colonial Period (ss. XVI-XVIII) and even during many decades of the Republic (ss. XIX and XX). However, many studies aimed at focusing on a physical characterization – the mechanical and chemical constituents of the materials are virtually nonexistent.

The Puente de calicanto or Puente Ortiz (Calicanto Bridge or Ortiz Bridge) was built in the city of Cali between 1835 and 1845 across a river with the same name. It was built under the initial direction of a citizen named Jose Montehermoso and later under the supervision of the Franciscan priest, José Ignacio Ortiz. At the time of its commissioning, the structure had five leveling arches and four bow arches over the river that were built entirely from common bricks, which were stuck together with mortar made from a mixture of lime, sand and water (Figure 1). A layer was also prepared from lime mortar and covered the outer walls of the bridge (spandrels) to protect the highly porous bricks from moisture.



Fig. 1. *Lateral view of a recent picture of Puente Ortiz in the city of Cali (Colombia).*  
[Drawing: E. Sotelo – Photo: J. Galindo]

Up until 1918, the structure did not experience any significant changes. Then, an expansion was conducted for the bearing extension board by incorporating concrete crossbeams. In 1945, two separate bridges were attached with concrete on each side of the original bridge and were buried under the ground to the extreme north and south of the nineteenth century original construction. In 2011, an urban archaeological excavation managed to unearth the walls of the southern end (approaches), which were in good condition, allowing them to obtain samples of the types of lime mortar used in both the bricks and the paste in the plaster of their spandrels (Figure 2).

2



Fig. 2. *Picture of the walls that form the southern end of Puente Ortiz in Cali during the process of archaeological excavation. Left: approach looking "upstream". Right: approach looking "downstream".* [Photo: J. Galindo]

### Experimental Details

Until 1970-1980, the characterization of historical mortars was mainly based on traditional chemical analyses performed using wetting methods (Elsen, 2006). Nevertheless, the interpretation of these results was difficult and often not possible without a complete understanding of the nature of the different components of the mortar used. This difficulty is the reason why most subsequent characterizations have been supported by the techniques of electron microscopy and X-ray diffraction, especially in the early stages of testing.

Other techniques, such as DSC/TGA and FTIR, have also been employed. In any case, the selection of the appropriate analysis technique depends primarily on the questions to be answered and on the amount of material that is available.

### Techniques employed in the characterization of historical mortars

Below is a brief description of the laboratory techniques used in this research:

- X-ray diffraction (XRD): used for the analysis of the components or the mineralogical crystalline phases that are present in the sample (Braga Reis, 1994) and provides valuable information for other types of analyses. In combination with a thermal analysis, XRD can answer a large number of questions, such as the type of agglomerates that exist and the presence of pozzolanic materials.

- Infrared Spectroscopy by Fourier Transform (FT-IR): reveals the compounds that have been developed in historical mortars during the years when curing and weathering processes took place (Maravelaki et al., 2005). In addition, this technique is capable of obtaining qualitative information from a chemical standpoint, particularly pertaining to the characteristic compounds contained in the mortar (calcium and magnesium hydroxides, carbonates, gypsum, etc.) This technique also helps determine the presence of salts (nitrates, sulfates, oxalates, etc.) and organic compounds.

- Differential scanning calorimetry (DSC): measures the heat flux to be supplied independently to a sample M contained in a crucible given a standard reference R to allow both of the measurements to follow the same temperature trend  $T_p(t)$ .

- Scanning electron microscopy (SEM) at room temperature: provides information on the mineral morphology, the crystal size, the chemical composition and the phases formed in the sample (Maravelaki et al., 2005).

### Sample extraction

To perform a differential analysis between the mortar paste of the bricks and the mortar of the plaster, samples were collected from each source via a manual procedure in which a flat chisel tip was used (Figure 3).



Fig. 3. *Sample extraction of the mortar paste at Puente Ortiz.*

[Photo: J. Galindo]

Three (3) mortar paste specimens were obtained from the approach that looks towards the east, and two (2) specimens were obtained from the approach that looks towards the west. The plastering mortar samples were obtained entirely from the approach that looks towards the west, in which a surface cloth of 4.00 m<sup>2</sup> was maintained in a good condition, with traces of the original yellow pigment (Figure 4).



Fig. 4. A sample extraction site of plaster mortar at Puente Ortiz  
[Photo: J. Galindo]

Table 1.

Lists the samples and the nomenclature used in the laboratory tests:

POMP-01	Puente Ortiz, Mortar Paste, Specimen 01
POMP-02	Puente Ortiz, Mortar Paste, Specimen 02
POMP-03	Puente Ortiz, Mortar Paste, Specimen 03
POMP-04	Puente Ortiz, Mortar Paste, Specimen 04
POMP-05	Puente Ortiz, Mortar Paste, Specimen 05
POMR-01	Puente Ortiz, Plaster Mortar, Specimen 01
POMR-02	Puente Ortiz, Plaster Mortar, Specimen 02

## Results

The following section describes the results of the various laboratory techniques used:

### *Macroscopic characteristics of the samples:*

The average density of the samples in both types of mortar (paste and plaster) at Puente Ortiz in Cali is 2.65 g/cm<sup>3</sup>, and the samples have a soft consistency and a dark color. They also have a high degree of humidity because the specimens have been buried for at least 70 years.

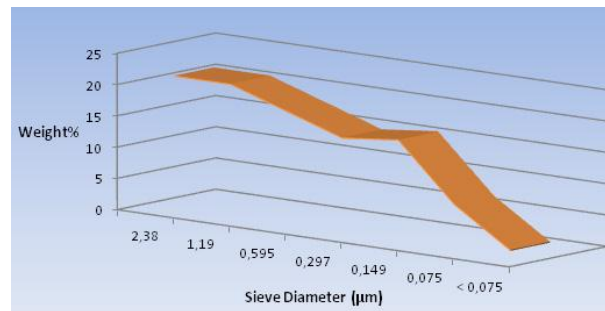
*Agglomerating proportion/aggregate and grain size distribution:*

The ratio of agglomerate (lime) to the aggregate (sand) is different for each type of mortar studied, as shown in Table 2:

Table 2.  
Agglomerate ratio in the historical mortars of Puente Ortiz.

	Agglomerate	Sand	Ratio
Mortar Paste	26.95%	73.04%	1 : 2.71
Plaster Mortar	34.6%	65.39%	1 : 1.89

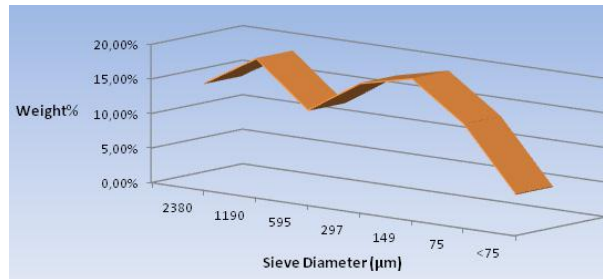
Figure 5 shows the grain size distribution for the mortar paste aggregate samples at Puente Ortiz in the city of Cali. A trend was observed in the granulometric analysis of sample POMP-03, corresponding to a bimodal distribution (approximately 1190 microns and 297 microns), with the descent trend starting with the grain size of 1190 microns. In the sample, the size of the finer particles (<75 microns) is less than 6% of the sample. Fifty percent of the grains fall within a high range between 1190 microns and 595 microns.



Sieve	Opening (µm)	% Kept
No. 8	2380	21
No. 16	1190	21
No. 30	595	18
No. 50	297	15
No. 100	149	16
No. 200	75	7
Depth	<75	1

Fig. 5. The grain size distribution for the samples of mortar paste at Puente Ortiz (POMP-03)

Figure 6 shows the grain size distribution of the sample plaster mortar at Puente Ortiz. The grain size distribution of the sand mortar sample POMR-02 shows a bimodal distribution (approximately 1190 microns and 149 microns) that is relatively homogeneous, where the size of the finer particles (<75 microns) is less than 6% of the sample. Approximately 50.12% of the grains fall within a low range between 595 microns and 75 microns. It is concluded that fine sand was used for the preparation of the mortar plastering and not for the mortar paste.



Sieve	Opening (µm)	% Kept
No. 8	2380	14
No. 16	1190	19
No. 30	595	12
No. 50	297	17
No. 100	149	19
No. 200	75	14
Depth	<75	5

Fig. 6. The grain size distribution for the samples of mortar plaster at Puente Ortiz (POMR-02)

*Mineralogical component present in the samples:*

Figure 7 shows the X-ray diffraction pattern for mortar paste sample POMP-02. The presence of quartz [SiO<sub>2</sub>] evidences the use of a quartzitic sand mortar in the original formulation (Table 3). Calcite [CaCO<sub>3</sub>] is indicative of the use of lime. By comparing the intensities, it can be established that the sample is rich in sand in relation to the content of calcite.

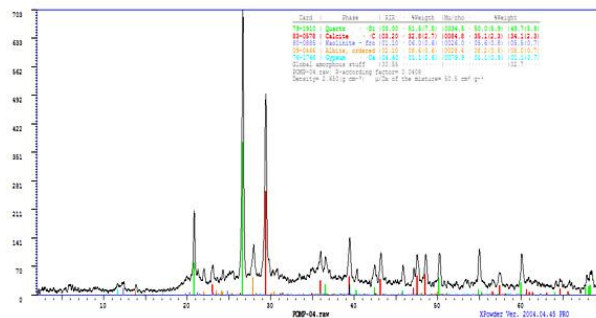


Fig. 7. X-ray diffraction for the mortar paste samples at Puente Ortiz in Cali (POMP-02).

Figure 8 shows the X-ray diffraction pattern for plastering mortar sample POMR-01. The presence of quartz [SiO<sub>2</sub>] evidences the use of quartzitic sand in the formulation of the original mortar (Table 3). Calcite [CaCO<sub>3</sub>] is indicative of the use of lime and its chemical transformation into calcium carbonate.

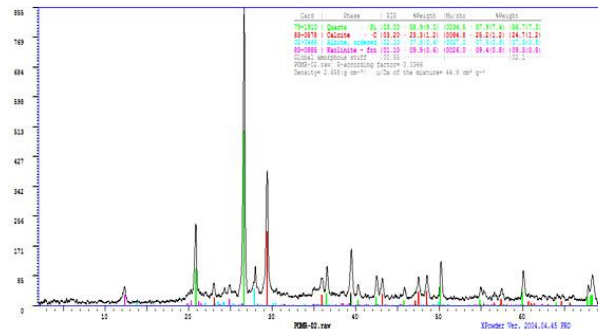


Fig. 8. X-ray diffraction for the mortar plaster samples at Puente Ortiz in Cali (POMR-01).

Table 3.  
XRD analysis for the mortar samples from Puente Ortiz.

	Mortar Paste	Mortar Plaster
Compound	% Weight	% Weight
Quartz [SiO <sub>2</sub> ]	51.50%	58.90%
Calcite [CaCO <sub>3</sub> ]	32.80%	23.30%
Kaolinite [Al <sub>2</sub> Si <sub>2</sub> O <sub>5</sub> (OH) <sub>4</sub> ]	6.00%	9.90%
Albite [NaAlSi <sub>3</sub> O <sub>8</sub> ]	8.60%	7.80%
Clay [CaSO <sub>4</sub> · 2H <sub>2</sub> O]	1.10%	-

The X-ray diffraction analysis established that no high temperature phases were obtained during the technological process of the manufacturing of the mortars. Therefore, burning of the limestone for the lime paste was performed at temperatures below 600 °C (because of the presence of kaolinite). The presence of kaolinite indicates that the limestone contained a certain amount of clay.

The use of limestone with clay is necessary because of the hydraulic characteristics that are required for bridge construction. Reports made by several authors (Elsen, 2006; Maravelaki et al., 2005) indicate a high pozzolanic reactivity resulting from the use of a kaolinitic clay, which promotes an increase in mechanical strength due to its possible activation in amorphous metakaolin. A lack of thermal activation of the clay material is observed.

#### Analysis by FT-IR:

Figure 9 shows the FT-IR spectrum of mortar paste sample POMP-03. The bands at 2514 cm<sup>-1</sup>, 1429 cm<sup>-1</sup>, 874 cm<sup>-1</sup> and 712 cm<sup>-1</sup> correspond to the three different modes of elongation of the C-O bonds. The thin band at 1796 cm<sup>-1</sup> is associated with the carbonate C-O bond. All of these bands allow for the identification of calcium carbonate (CaCO<sub>3</sub>).

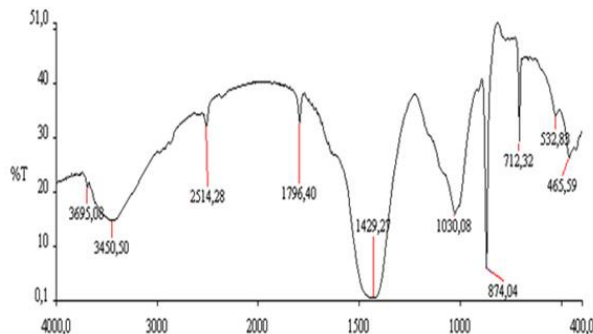


Fig. 9. Spectroscopy of the mortar paste samples at Puente Ortiz in Cali (POMP-03).

The bands at 3450 cm<sup>-1</sup> and 1628 cm<sup>-1</sup> can be explained by the presence of the hydroxide ions in water (Genestar, Pons & More, 2006). The water could have been subject to hydraulic compounds, such as silicate and aluminate hydrates (Silva & Wenk Monteiro, 2005). The band at 532 cm<sup>-1</sup> may indicate the presence of oxides. The bands at 1030 cm<sup>-1</sup> and 465 cm<sup>-1</sup> indicate the presence of quartz (Maravelaki et al., 2005).

Figure 10 shows the FTIR spectra for plastering mortar sample POMR-02. The bands at 1431 cm<sup>-1</sup>, 874 cm<sup>-1</sup> and 712 cm<sup>-1</sup> correspond to the three different stretching modes of the CO bonds. The narrow and intense band at 1796 cm<sup>-1</sup> is associated with a carbonate CO bond. The bands at 3453 cm<sup>-1</sup> and 1622 cm<sup>-1</sup> can be explained by the presence of the hydroxide ions in water (Genestar, Pons & More, 2006). The water could have been subject to hydraulic compounds, such as silicate and aluminate hydrates (Silva & Wenk Monteiro, 2005).

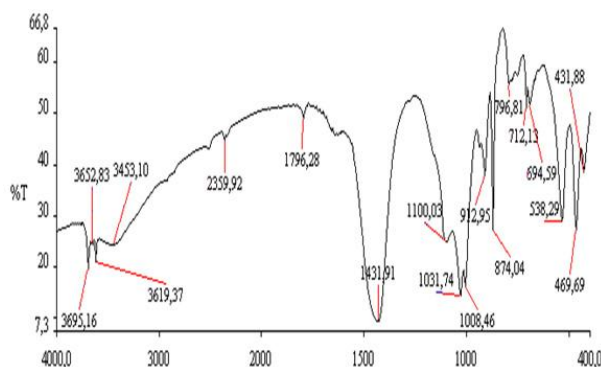


Fig. 10. Plaster mortar sample (POMR-02) spectroscopy at Puente Ortiz in Cali

The band at 538 cm<sup>-1</sup> may indicate the presence of an oxide (Genestar, Pons & More, 2006). The bands at 1100 cm<sup>-1</sup>, 1031 cm<sup>-1</sup>, 796 cm<sup>-1</sup> and 469 cm<sup>-1</sup> indicate the presence of quartz (Maravelaki et al., 2005). The vibrations at 1008 cm<sup>-1</sup> could indicate the presence of silicoaluminate hydrates.

#### Analysis by differential scanning calorimetry

The DSC curve of mortar paste sample POMP-03 is shown in Figure 11. The analysis indicates a pure lime mortar. Typically, most of the plaster consists of calcite [CaCO<sub>3</sub>] without the presence of

hydraulic components because they are hygroscopic and because no significant endothermic peak in the range of 100-450 °C was observed. This analysis allows for the differentiation of the hydraulic mortars from the lime mortars in which the latter contains smaller amounts of absorbed water (Bakolas et al., 1998).

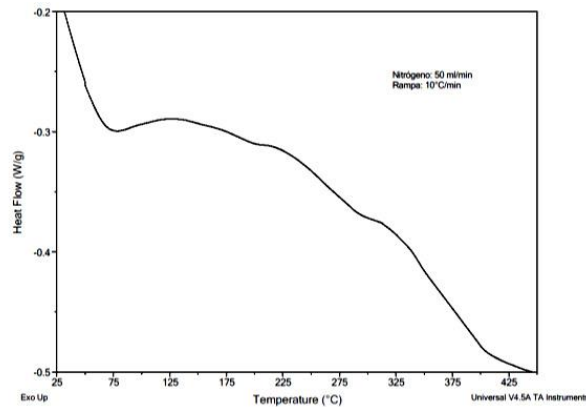


Fig. 11. *Differential scanning calorimetry of the mortar paste sample at Puente Ortiz (POMP-03).*

The thermal analysis indicates the presence of a limited amount of clay minerals. The insignificant endothermic effects at 200 °C, 292 °C and 408 °C can be attributed to small amounts of silicate and aluminate in the sample. The thermal transition at 78 °C indicates the presence of hygroscopic water. The endothermic peak at 408 °C indicates the dehydration of kaolinite.

9

The DSC curve of mortar plaster sample POMR-02 is shown in Figure 12. The spectrum shows a lime mortar, which typically has a very small number of hydraulic components. Three significant endothermic reactions are also observed at 202 °C, 302 °C and 405 °C, which may indicate the dehydration of a compound containing aluminum hydraulic and/or silicon. The endothermic peak at 77 °C indicates the presence of hygroscopic water. A weak endothermic reaction in the curve indicates the reorganization of the octahedral sheets of kaolinite at 302 °C, as demonstrated by Kakali et al. (2001).

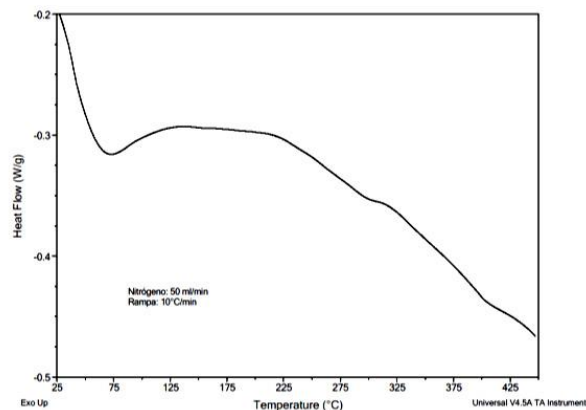


Fig. 12. *Differential scanning calorimetry of the plaster mortar samples at Puente Ortiz in Cali (POMR-02).*

### *Analysis by scanning electron microscopy*

An image obtained using scanning electron microscopy for mortar paste sample POMP-03 is shown in Figure 13. The observations made by SEM show grains of sand with approximately 1 mm diameters, the surface layers of which are covered with fine powders, particularly CaCO<sub>3</sub>. Below these fine powders is a high concentration of solid grains with low porosity, which do not show cracks or fractures. The limits observed between the larger particles appear to have a good grip.

The chemical composition of the large particles showed a higher content of silicon and aluminum in accordance with the energy dispersive spectrometry (Figure 14) analysis. The XRD analysis indicates that the main component of the large particles is quartz (SiO<sub>2</sub>), and a major component of fine particles is calcite. Larger solid particles indicate that the material is mechanically strong. The larger particles appear to be connected through the fine powders.

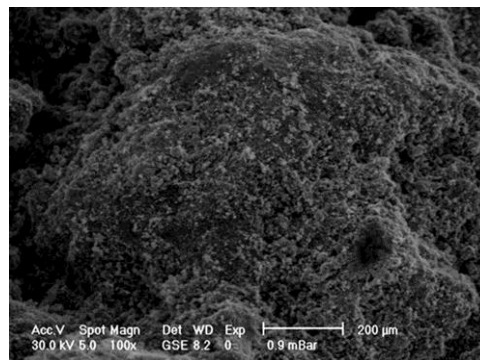


Fig. 13. *Scanning electron microscopy of the mortar paste samples at Puente Ortiz in Cali (POMP-03).*

Amplification of the fine powders allows us to observe the irregular morphology of the CaCO<sub>3</sub> crystals derived from the carbonation of the lime, which show an inhomogeneous grain size distribution ranging from 870 nm to approximately 5 microns. The size and texture of the calcite grains are formed according to the environmental conditions of carbonation. The material obtained from the pozzolanic reaction by-products is not readily identifiable (Elsen, 2006). No fibers, which would improve the mechanical behavior of the material, are observed.

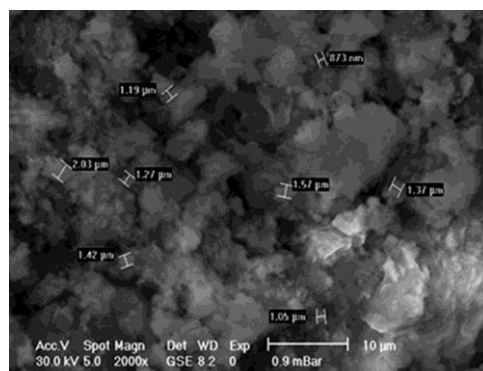


Fig. 14. *Scanning electron microscopy of the sample of mortar paste at Puente Ortiz in Cali (POMP-03).*

The SEM-EDS microanalysis (Figure 15) mainly identifies the elements of Ca, Si and Al, thus confirming the presence of the relevant compounds of the mortar, such as calcite, quartz and Al, indicating the presence of clay compounds. In addition, other elements are identified indicating the presence of impurities, such as Fe.

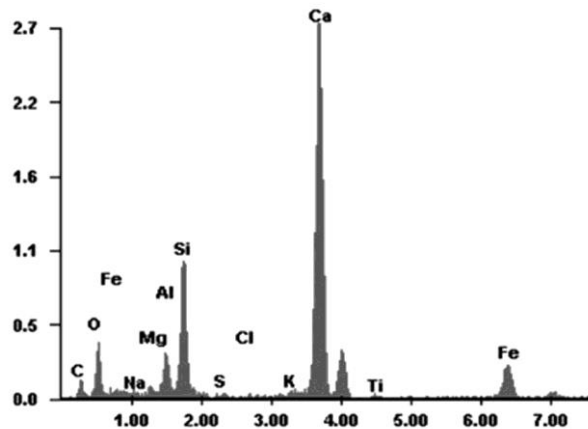


Fig. 15. The EDS analysis of the mortar paste samples at Puente Ortiz (POMP-03).

The scanning electron microscopy of plastering mortar samples POMR-02 is shown in Figure 16. The figure shows a surface layer of powders of calcite coated with quartz grains that provide a connection between them. These powders almost completely fill the spaces between the sand particles, which is a feature that determines the low permeability to the masonry interior, thus preserving harmful agents such as atmospheric CO<sub>2</sub> and H<sub>2</sub>O.

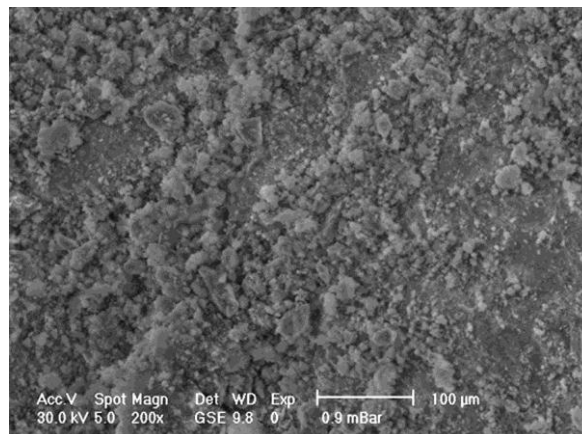


Fig. 16. Scanning electron microscopy of the plaster mortar samples at Puente Ortiz in Cali (POMR-02).

Few pores are observed (Figure 17), which were possibly formed during curing and carbonation. Good compaction of the powders is also observed. No fibers or gels are observed, indicating a calcium silicate hydrate phase (CSH), which usually crystallizes on the surface. This finding confirms that the clay material failed to be activated.

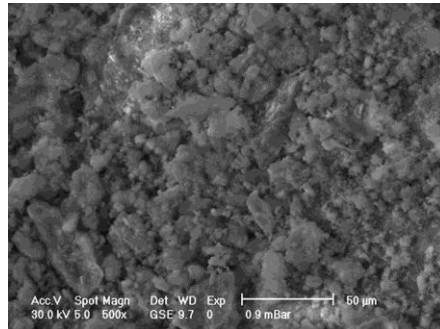


Fig. 17. Scanning electron microscopy of the plaster mortar samples at Puente Ortiz in Cali (POMR-02).

A chemical mapping (Table 4) of the surface primarily identifies elements Si, Ca and Al (Figure 18). The chemical composition of the large particles showed higher contents of Si and Al in accordance with the energy dispersive spectrometry (EDS) analysis. The main element of the fine particles is Ca.

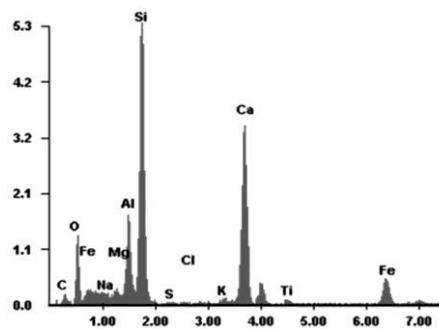


Fig. 18. The EDS analysis for mortar plaster samples at Puente Ortiz in Cali (POMR-02).

Table 4

The EDS analysis for the mortar paste and mortar plaster samples at Puente Ortiz in Cali

Element	Mortar paste		Mortar plaster	
	Weight %	Atomic %	Weight %	Atomic %
Ca	40.59	25.24	21.43	12.44
O	22.2	34.59	23.38	34
Si	10.32	9.15	23.24	19.25
C	9.69	20.11	10.06	19.49
Al	3.91	3.61	7.91	6.82
Fe	10.23	4.56	8.85	3.69
S	0.27	0.21	0.18	0.13
Mg	1.15	1.18	1.52	1.46
K	0.46	0.3	0.65	0.39
Na	0.74	0.81	1.81	1.83
Cl	0.11	0.08	0.18	0.12
Ti	0.32	0.17	0.78	0.38
Total	100	100	100	100

## Conclusion

The methodology used in this study emphasizes the complementary character of the different characterization techniques: X-ray diffraction to identify the main crystalline phases; FT-IR for an evaluation of the non-crystalline phase; SEM at room temperature for an evaluation of the morphology; and DSC to determine the nature of the clay mortars.

The empirical builders of the nineteenth century prepared paste mortars and plaster mortars differently according to specific proportions: a higher content of sand (coarse aggregate) in the first case and a greater amount of lime (fine aggregate) in the latter case.

The size analysis shows that the homemade lime (produced at temperatures below 600 °C) used in the mortar paste was thicker than that of the plaster mortar and had favorable effects on the mechanical properties (strength).

The results converge to reveal the calcitic nature of the mortar used in both of the bridges, confirming the widespread use of lime in the preparation of the mortar at that time, and indicate a lack of the use of fibers and materials of organic origin for its preparation.

The lime mortar used in the paste and plaster at Puente Ortiz reveals a low presence of clay, indicating that a careful process was used by their builders in the selection of raw materials.

## Acknowledgements

The authors express their gratitude to archaeologists Sonia Blanco and Nathalia Robayo at the Scientific Research Institute of Cauca Valley (INCIVA), who were responsible for the excavation of the remains of Puente Ortiz and provided access to its archaeological sites. The authors acknowledge Mr. Vicente Benavides Palacios, who supported the characterization by X-ray diffraction.

## References

- Bakolas, A., Biscontin, G., Moropoulou, A. & Zendri, E. (1998 ). Characterization of structural Byzantine mortars by thermogravimetric analysis. *Thermochim. Acta* (321), 151– 160.
- Braga Reis, M.O. (1994). *Difracção de Raios X [X-ray diffraction]. Curso Técnicas de Caracterização Química e Físico-Química de Materiais*. Lisboa: LNEC.
- Elsen, J. (2006). Microscopy of historic mortars – a Review. *Cement and Concrete Research* (36), 1416 - 1424.
- Genestar, C., Pons, C. & Más, A. (2006). Analytical characterisation of ancient mortars from the archaeological Roman city of Pollentia (Balearic Islands, Spain). *Analytica Chimica Acta* (557), 373 - 379.
- Kakali, G., Perraki, T., Tsvivilis, S. & Badogiannis, E. (2001). Thermal treatment of kaolin: the effect of mineralogy on the pozzolanic activity. *Applied Clay Science* (20), 73-80.
- Maravelaki, P., Bakolas, A., Karatasios, I. & Kilikoglou, V. (2005). Hydraulic lime mortars for the restoration of historic masonry in Crete. *Cement and Concrete Research* (35), 1577 - 1586.
- Silva, D., Wenk, H., & Monteiro, P. (2005). Comparative investigation of mortars from Roman Colosseum and cistern. *Thermochimica Acta* (438), 35 - 40.